# Simulation of Ultra-low Cycle Fatigue Failure of Reduced Beam Section Specimen

Graduate School of Science and Engineering, Ehime University — ○ S.C. Siriwardane (Student Member)
Department of Civil and Environmental Engineering, Ehime University — Mitao Ohga (Member)
Department of Civil and Environmental Engineering, Ehime University — Kazuhiro Taniwaki (Member)

## 1. Introduction

The concept of ultra-low cycle fatigue (ULCF) was originated in year 2005 with some of sudden failures of existing structures, which were characterized by large scale cyclic yielding due to occasional loadings such as earthquakes, typhoons. Generally, experimental approaches are popular for ULCF failure prediction. As for the authors view, only one theoretical study has been published in year 2005 (Kanvinde et al., 2005) and found related applications are very less. Therefore, this paper basically describes the application procedure of the described criteria to predict the real ULCF failure. The comparison of theoretically predicted failure with experimentally predicted failure is mainly considered for a test specimen which is generally used to simulate failure of reduced beam section (RBS) type connections.

## 2. Reduced beam section type connection

During the Northridge and Kobe earthquake, welded connections in steel moment frames were found to be a weak link in structural systems (Chi et al., 2006 and Kanvinde et al., 2006, Carden et al., 2006). After these disasters, RBS or dog-bone type connection detail (see Fig. 1) was developed to concentrate the plastic hinge a certain distance away from the connection within the beam. Though such connections have the potential to prevent sudden and brittle failures such as those in welded connections, there is always the possibility of ductile fracture under large plastic strains. Therefore, it is advisable to evaluate the ULCF strength of these connections to avoid sudden failures.

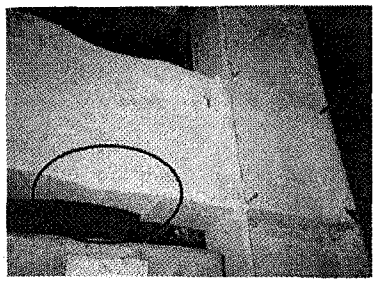

Fig 1. RBS type welded connection

## 3. Failure Criterion for Ultra-Low Cycle Fatigue

The ULCF has been introduced to distinguish it from low cycle fatigue. The observed failure mechanism is based on voids growth and the failure criterion is summarized as,

$$\bar{\varepsilon}_*^p > \exp(-\lambda\bar{\varepsilon}^p).\bar{\varepsilon}_{critical}^p \quad (1)$$

The $\bar{\varepsilon}_*^p$ is significant plastic strain. The $\lambda$ is material damageability parameter. The $\bar{\varepsilon}^p$ is the effective plastic strain and $\bar{\varepsilon}_{critical}^p$ is the critical effective plastic strain at monotonic failure. Following section describes a methodology to predict ULCF failure of a real structure.

## 4. Proposed Methodology to Predict ULCF Failure

The proposed method consists of four major steps.

*Step 1: Determination of critical effective plastic strain*

According to the monotonic ductile failure criterion (Chi et al., 2006), the effective plastic strain ($\bar{\varepsilon}^p$) is equal to the critical effective plastic strain ($\bar{\varepsilon}_{critical}^p$) when ductile failure happens as shown bellow.

$$\bar{\varepsilon}^p - \alpha \exp\left(-1.5\frac{\sigma_m}{\sigma_e}\right) > 0 \quad (2)$$

There, it is important to consider a zone that has higher probability of failure. In finding of this zone, one can select areas where effective stresses are present and such higher effective stress area is called as "critical zone". Having found this area, critical effective plastic strain ($\bar{\varepsilon}_{critical}^p$) should be found for each Gauss points of this critical zone.

*Step 2: Determination of critical significant plastic strain*

Once the critical effective plastic strains due to monotonic loading at each sampling locations in critical zone are determined, the cyclically degraded values of the critical monotonic effective plastic strain (usually called as critical significant plastic strain) at that zone is calculated at the beginning of each tensile cycle for each sampling location using following equation,

$$\bar{\varepsilon}_{*critical}^p = \exp(-\lambda\bar{\varepsilon}^p).\bar{\varepsilon}_{critical}^p \quad (3)$$

For clearness of understanding the behavior it is better to plot the critical significant plastic strain ($\bar{\varepsilon}_{*critical}^p$) versus locations in particular critical zone for considered loading steps. As for an example, when the critical zone becomes a nearly straight-line, plot has to be done critical significant plastic strain ($\bar{\varepsilon}_{*critical}^p$) versus distance along the line.

*Step 3:Determination of significant plastic strain*

The significant plastic strains at the critical zone can be calculated during the FE analysis simultaneously with step 2 using the following relations. $T$ is triaxiality and $n$ is the loading step number,

$$\text{When } T > 0;\ (\bar{\varepsilon}_t^p)_{(n+1)} = (\bar{\varepsilon}_t^p)_n + (d\bar{\varepsilon}^p)_n \quad (4)$$

$$\text{When } T < 0;\ (\bar{\varepsilon}_c^p)_{(n+1)} = (\bar{\varepsilon}_c^p)_n + (d\bar{\varepsilon}^p)_n \quad (5)$$

Subtracting Eq. (4) from Eq. (5) the applied significant plastic strain at sampling location in critical zone is calculated as,

$$(\bar{\varepsilon}_*^p)_{n+1} = (\bar{\varepsilon}_t^p)_{n+1} - (\bar{\varepsilon}_c^p)_{n+1} \quad (6)$$

*Step 4: The $(\bar{\varepsilon}_*^p - \bar{\varepsilon}_{*critical}^p)$ plot and crack initiation*

This $(\bar{\varepsilon}_*^p - \bar{\varepsilon}_{*critical}^p)$ is the difference between the applied significant plastic strain $(\bar{\varepsilon}_*^p)$ and the critical significant plastic strain $(\bar{\varepsilon}_{*critical}^p)$, and it is somewhat similar to the ductile failure criteria. Failure is assumed to have occurred at a point when this quantity is greater than zero. A prediction of ULCF crack initiation is made when this quantity exceeds zero over the characteristic length ($l^*$) along the critical zone.

## 5. Theoretical Prediction of ULCF failure

Considering symmetricity of RBS specimen (see Fig 2) geometry, loading and boundary conditions, the one-fourth of the geometry was subjected to FE analysis. The nine-node shell element was used for FE mesh as shown in Fig 3.

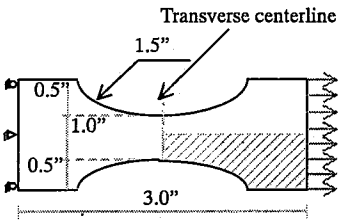

Hatched area is subjected to FE analysis

Fig 2. Geometry of RBS specimen

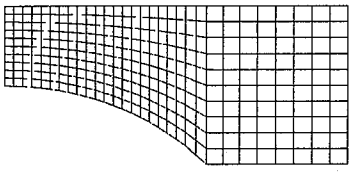

Fig 3. FEM mesh

As following the methodology in section 4, Initially considered geometry is subjected to the monotonic load analysis. By observing the stress distribution at ductile failure (stress contour is shown in Fig 4), it is able to conclude that critical zone lies along the transverse centerline of the specimen as shown in Fig 4. The considered material is, A572-grade 50 steel and toughness index ($\alpha$) was taken as 1.18. Hence the critical effective plastic strain ($\bar{\varepsilon}^p_{critical}$) at monotonic loading is calculated for sampling Gauss points along the transverse centerline of the specimen.

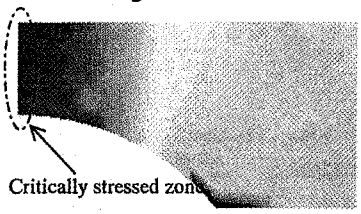

Fig 4. von Mises stress contour

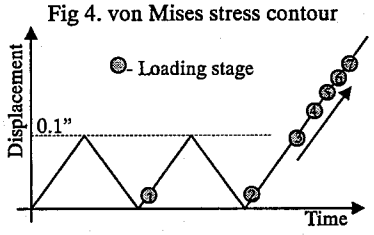

Fig 5. Loading history (quasi-static)

Then cyclic load FE analysis was conducted for one-fourth part of the specimen. The applied load versus (displacement) time variation is indicated in Fig 5 and it has been predicted to simulate same effect of the experimental cyclic load test. Damaged critical significant plastic strain variations are plotted at different loading stages as shown in Fig 6. Simultaneously the applied significant plastic strain also calculated for sampling Gauss points. Hence the $(\bar{\varepsilon}^p_* - \bar{\varepsilon}^p_{*critical})$ variations along the transverse centerline were determined and plotted as Fig 7. Finally the prediction of ULCF macro crack initiation is made when $(\bar{\varepsilon}^p_* - \bar{\varepsilon}^p_{*critical})$ exceeds zero over the characteristic length ($l^*$) at loading stage 7. The corresponding displacement to this instant is recorded as the failure displacement, and the theoretical prediction of ULCF failure is compared with experimental results as shown in Table 1. Both corresponding load displacement relations are drawn in Fig 8.

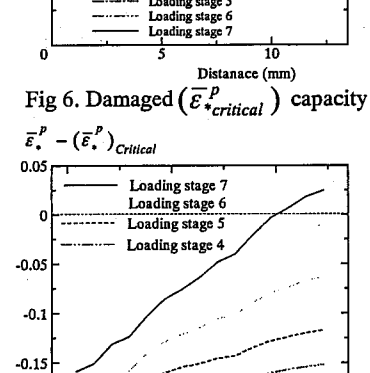

Fig 6. Damaged $(\bar{\varepsilon}^p_{*critical})$ capacity



Fig 7. $\bar{\varepsilon}^p_* - (\bar{\varepsilon}^p_*)_{Critical}$ variation

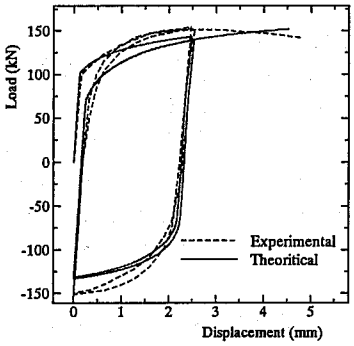

Fig 8. Load/ displacement comparison

Table 1: Comparison of displacement and effective stresses

| Description | Ductile failure | ULCF failure | |
|---|---|---|---|
| | | Test | Theoretical |
| Failure displacement | 6.23 mm | 4.76 mm | 4.55 mm |
| Maximum stress | 667 MPa | No | 572 MPa |

## 6. Conclusions

The Fig 8 shows that theoretical prediction of ULCF failure is safe side of the real failure. Therefore it is possible to express that described theoretical ULCF failure criterion provide more optimized prediction to real failure of RBS type connection.

In advance, the Table 1 shows that same specimen is subjected to fail with lesser amount of displacement or effective stresses than ductile failure. Therefore, it reveals that even though the structure already designed to prevent ductile failure due to seismic loading (this is considered as the seismic design check for structural details in present day) it may fail due to the effect of ULCF failure by receiving lesser amount of applied displacement or stress. As a result of that, it can be emphasized that the ductile failure check is not only sufficient but also ULCF failure check is required for seismic design of structural details to prevent the sudden failures.

## References


Carden, L.P., Itani, A.M., and Buckle, L.G. (2006). Seismic performance of steel girder bridges with ductile cross frames using single angle X braces. *Jou. of Structural Engineering*, ASCE, 132(3), 329-337.

Chi, W.M., Kanvinde, A.M., and Deierlein, G.G. (2006). Prediction of ductile fracture in steel connection using SMCS criterion. *Jou. of Structural Engineering*, ASCE, 132(2), 171-181.

Kanvinde, A.M., and Deierlein, G.G. (2005). Continuum-based micro models for ultra-low cycle fatigue crack initiation in steel structures. *Proceedings, ASCE Structures Congress and Exposition,* New York, NY.

Kanvinde, A.M., and Deierlein, G.G. (2006). Growth model and stress modified critical strain model to predict ductile fracture in structural steels. *Jou. of Structural Engineering*, ASCE, 132(12), 1907-1918.